



# Discovery of New Inhibitors of Aldose Reductase from Molecular Docking and Database Screening

Giulio Rastelli,\* Anna Maria Ferrari, Luca Costantino and Maria Cristina Gamberini

*Dipartimento di Scienze Farmaceutiche, Università di Modena e Reggio Emilia, Via Campi 183, 41100 Modena, Italy*

Received 28 June 2001; accepted 19 November 2001

**Abstract**—Aldose reductase (ALR2) is a target enzyme for the treatment of diabetic complications. Owing to the limited number of currently available drugs for the treatment of diabetic complications, the discovery of new inhibitors of ALR2 that can potentially be optimized as drugs appears highly desirable. In this study, a molecular docking analysis of the structures of more than 127,000 organic compounds contained in the National Cancer Institute database was performed to find and score molecules that are complementary to ALR2. Besides retrieving several carboxylic acid derivatives, which are known to generally inhibit aldose reductase, docking proposed other families of putative inhibitors such as sulfonic acids, nitro-derivatives, sulfonamides and carbonyl derivatives. Twenty-five compounds, chosen as the highest-scoring representatives of each of these families, were tested as aldose reductase inhibitors. Five of them were found to inhibit aldose reductase in the micromolar range. For these active compounds, selectivity with respect to the closely-related aldehyde reductase was determined by measuring the corresponding inhibitory activities. The structures of the complexes between the new lead inhibitors and aldose reductase, here refined with molecular mechanics and molecular dynamics calculations, suggest that new pharmacophoric groups can bind aldose reductase very efficiently. In the case of the family of the nitro-derivative inhibitors, a class of particularly interesting compounds, a round of optimizations was performed with the synthesis and biological evaluation of a series of derivatives aimed at testing the proposed binding mode and at improving interaction with active site residues. Starting from a hit compound having an  $IC_{50}$  of 42  $\mu$ M, the most potent compound synthesized showed a 10-fold increase in inhibitory activity and 10-fold selectivity with respect to ALR1, and structure–activity relationships of the designed compounds were in agreement with the proposed mode of binding at the active site. © 2002 Elsevier Science Ltd. All rights reserved.

## Introduction

Aldose reductase (alditol/NADP<sup>+</sup> oxidoreductase, E.C.1.1.1.21, ALR2) is the first enzyme of the polyol pathway which reduces excess D-glucose into D-sorbitol with concomitant conversion of NADPH to NADP<sup>+</sup>.<sup>1–4</sup> The polyol pathway plays an important role in the development of degenerative complications of diabetes. The association between hyperglycaemia and the development of long-term diabetic complications such as neuropathy, retinopathy and cataract is well documented.<sup>5</sup> At elevated blood glucose levels, such as those occurring during diabetes, a significant flux of glucose through the polyol pathway is induced in tissues like nerves, retina, lens and kidney, and the activation of this pathway is believed to induce the appearance of diabetic complications affecting various pathogenic factors. Aldose reductase inhibitors therefore offer the possibility of safely preventing or arresting the progression of long-term diabetic complications, despite

imperfect control of blood glucose and with no risk of hyperglycaemia.

To date, two main classes of orally-active aldose reductase inhibitors (ARIs) have been reported: spirohydantoins and carboxylic acids, with Sorbinil and Tolrestat being the most representative members of each family, respectively. In general, while the *in vitro* activity of spirohydantoins and carboxylic acid ARIs is similar, their *in vivo* activity is very different. *In vivo*, carboxylic acids possess lower activity than spirohydantoins,<sup>6,7</sup> a finding that is likely attributable to their lower  $pK_a$  and to a resultant impairment in penetrating physiological membranes. Spirohydantoins, on the other hand, which show higher activity *in vivo*, have clearly proved to cause hypersensitivity reactions.<sup>4,8</sup> On these grounds, there is an urgent need to discover and develop new lead ARIs not related to spirohydantoins or carboxylic acids, and preferably with  $pK_a$  values higher than those of carboxylic acids.

Molecular docking and ‘de-novo’ design are widely applied to the discovery of enzyme inhibitors with spe-

\*Corresponding author. Tel.: +39-059-205-5145; fax: +39-059-205-5131; e-mail: rastelli.giulio@unimo.it

cific and desired chemical properties.<sup>9–12</sup> One efficient approach to the design of new lead inhibitors is to select, within structural databases of several thousands of known and available organic molecules, those compounds that display the highest steric and electrostatic complementarity with the site of action.<sup>13–15</sup> In this context, the docking of 3-D-databases of organic molecules into the crystal structures of enzymes provides an efficient way of rationally selecting small subsets of interesting and promising candidates for biological testing.

Here, we report the results of a molecular docking study of the National Cancer Institute (NCI) database of organic molecules into the crystal structure of aldose reductase. After the screening of the entire database, which contained more than 127,000 compounds, only 25 were selected and evaluated as aldose reductase inhibitors. As will be shown, this study led to the discovery of families of ARIs not belonging to the classes of carboxylic acids or spirohydantoin. For one family of particular interest, a series of derivatives was designed and synthesized in order to test the proposed binding mode and to improve the interaction with active site residues. Finally, the selectivity for aldose reductase with respect to aldehyde reductase (ALR1),<sup>4</sup> an enzyme closely related to aldose reductase but not involved in diabetic complications, was determined by measuring the ALR1-inhibitory activity of the more active compounds here discovered.

### Strategy

Docking requires that the 3-D-structures of both the target enzyme and the ligands are known and available. To date, the Protein Data Bank contains several crystal structures of ALR2, both alone and complexed with known inhibitors. Crystallographic analysis of human ALR2 complexed with two carboxylic acid inhibitors, Zopolrestat<sup>16</sup> and citrate,<sup>17</sup> has provided important insights into the identification of the inhibitor binding site. Both complexes show that the inhibitors bind at the substrate active site, the carboxylate functional group of the inhibitors being close to the nicotinamide C4 carbon of NADP<sup>+</sup> and giving three hydrogen bonds with Tyr48, His110 and Trp111, three key residues for binding at the substrate active site of ALR2.<sup>18</sup> These latter residues and the positively charged nicotinamide ring of the oxidized cofactor form a positively charged binding site that recognizes and binds negatively charged inhibitors like carboxylates. Besides interaction with Tyr48, His110 and Trp111, Zopolrestat establishes a huge number of hydrophobic contacts with the enzyme. More recently, the crystal structures of porcine ALR2 complexed with Tolrestat, a different carboxylic acid inhibitor, and Sorbinil, a well-known member of the spirohydantoin family, have been described.<sup>19</sup> The hydantoin ring of Sorbinil binds at the active site within hydrogen bonding distances to Tyr48, His110 and Trp111, and resembles the interactions previously described for carboxylates. Recently, the sulfonyl-glycine inhibitor IDD384 was soaked into both human<sup>20</sup>

and porcine<sup>21</sup> ALR2. Interestingly, the binding of the inhibitor's hydrophilic head to Tyr48 and His110 was different in the two enzymes, the difference being attributed to a change in the protonation state of the inhibitor when soaked into the human (at pH 5.0) or pig lens (at pH 6.2) crystals. These studies point to the importance, in drug design, of considering the  $pK_a$  of the inhibitors and their possible protonation state at physiological pH.<sup>20</sup>

One interesting feature revealed by the binding of Zopolrestat is that it induces large conformational changes near the C-terminal end of the enzyme. After conformational changes, the benzothiazole substituent of the inhibitor is found to occupy a hydrophobic pocket, lined by Trp111 and Leu300, which is completely closed in the crystal structure of the holoenzyme, but which becomes accessible after conformational changes of a loop (residues 121–135) and a short segment (residues 298–303). Structure-based design of inhibitors different from Zopolrestat have further proved that the opening of this additional hydrophobic pocket and consequent binding of benzothiazole substituents lead to high-affinity inhibitors.<sup>22</sup> Furthermore, the opening of the additional hydrophobic pocket has important consequences for the selectivity of inhibitors with respect to the closely related aldehyde reductase (ALR1), since residues involved in the opening/closing of this pocket are the least conserved of the two related enzymes.<sup>19</sup>

The strategy devised for the discovery of new ALR2 inhibitors was as follows. In the first stage, the more than 127,000 structures of organic molecules from the NCI database were docked into the 3-D structure of ALR2 with the open additional hydrophobic pocket, using the program DOCK. This structure was preferred over the structures of the holoenzyme, and of other structures of ALR2-inhibitor complexes in which the hydrophobic pocket is closed, because of its potential to bind extra-aromatic substituents that enhance interaction with ALR2, increase inhibitory activity and increase selectivity with respect to ALR1. The aldose reductase structure used for docking is the one previously obtained by docking and energy minimization of a complex between ALR2 and a carboxylic acid inhibitor carrying a benzothiazole substituent.<sup>22</sup> This structure has the open additional hydrophobic pocket and is very similar to the structure of aldose reductase that binds Zopolrestat, whose coordinates are still not completely available (only the backbone atoms and the inhibitor are present in the Protein Data Bank, entry code 1MAR<sup>16</sup>). After docking, compounds displaying steric and electrostatic complementarity with the binding site were then saved. In this first stage, the 1270 best scoring compounds were saved, corresponding to a reduction to 1% of the original 127,000 structures in the database. Even though docking scores simply expressed as the sum of the electrostatic and the van der Waals interaction energies between a protein and a ligand are known to correlate poorly with inhibitory activity,<sup>23–25</sup> they are straightforward indices of complementarity for a database search. During the second stage, which con-

sisted in the clustering of the 1270 compounds into chemical families through the visualization of the ALR2–inhibitor complexes, a further selection was made. The molecules were clustered according to the functional group interacting with Tyr48 and His110, which are the most important residues in the active site. This choice follows the evidence that inhibition of ALR2 strongly depends upon the presence of a polar group bonded to these two residues (like the COO<sup>−</sup> of the carboxylic acid ARIs). Within each family, the compounds that displayed the highest scores and that satisfied the ‘minimal’ requisites for inhibition, that is the formation of hydrogen bonds with Tyr48 and His110, and the presence of a hydrophobic-aromatic fragment inserted into the additional hydrophobic pocket, were selected. Of the 1270 molecules deriving from the first stage, 25 were finally selected. For the molecules that were not commercially available, we searched the Available Chemical Directory (ACD) chemical catalogs for very similar compounds, using ChemFinder. In this stage, we made sure that changes introduced into the original structures did not alter their ability to bind the key residues of the active site. The modified compounds typically differed from the original hits by a few substituents not involved in direct recognition and binding of key aminoacids, and not in steric conflict with the enzyme. They were docked again into ALR2, to ensure that the structural modification of the hits did not significantly affect the orientation and the score. Since a 3-D version of the ACD was not available in our lab at the time this study was undertaken, a straightforward docking analysis of the ACD could not be performed.

The ALR2 inhibitory activity of the 25 candidates was determined and, for the compounds that proved active, selectivity with respect to the closely related enzyme aldehyde reductase (ALR1) was also determined.

Since the molecular docking procedure we used is rigid, that is it does not take into account the fact that both the enzyme and the molecule can change conformation after binding, the structures of the ALR2–inhibitor complexes were optimized using a molecular mechanics force-field (AMBER), and a molecular dynamics simulation protocol at  $T = 300$  K was applied as described in the experimental part. Very recently, Claußen et al. presented a new software, FlexE, which addresses the problem of protein-structure variation during docking by using an ensemble of different protein structures which represent the flexibility, and tested the software on Sorbinil, Tolrestat and Zopolrestat binding to ALR2.<sup>26</sup> Interestingly, the authors found that Tolrestat and Zopolrestat, which are the inhibitors that induce the opening of the additional hydrophobic pocket, could be docked in the correct orientation only by using their own ALR2 structures (with the open hydrophobic pocket). This points to the need to use different protein structures during docking, as the authors suggest.<sup>26</sup> In our case, however, the aim was to specifically target the ALR2 structure with the open additional hydrophobic pocket, for the reasons stated above, and docking was performed only on this structure. Then, to take into

account the induced-fit effects upon binding of diverse inhibitors, we devised an approach based on molecular dynamics simulations. Moreover, this choice allowed us to include the solvation effects at this stage, as the active site was fully solvated with water molecules prior to molecular dynamics.

Finally, for the most interesting of the families of bioactive compounds that emerged from docking, a round of optimization was undertaken with the synthesis and biological evaluation of a series of new derivatives specially designed to test the proposed binding mode and to improve interaction with active site residues.

## Results and Discussion

As a matter of validation of the docking procedure used throughout, Zopolrestat was first docked into the structure of ALR2. The highest-score orientation found by docking (with a score of  $-49$  kcal/mol) was found to be in full agreement with the crystal structure of the ALR2–Zopolrestat complex,<sup>16</sup> the docked orientation and the orientation in the crystal structure being closely superimposable. Docking of the entire NCI database of compounds into the ALR2 structure was then performed.

Before restricting the selection of the compounds to the actual number of candidates here tested, the 1270 best-scoring compounds identified by DOCK were analyzed. The analysis of the best scoring compounds and the visualization of the corresponding enzyme–inhibitor complexes revealed that molecules could be easily clustered into chemical families depending on the functional group interacting with Tyr48 and His110. This finding is intriguing, since these two residues are known to be of prime importance for the binding of inhibitors. Among the chemical families that DOCK orients in the proximity of Tyr48 and His110, we found carboxylic acids, sulfonic acids, nitro-derivatives, sulfonamides, and carbonyl derivatives able to form strong hydrogen bonds with the above-mentioned residues of ALR2. It is not surprising that among the highest scoring compounds we find several carboxylic acid derivatives, since their ability to inhibit ALR2 is known. Among the high scoring compounds, docking also selected glucose-6-phosphate, a molecule known to be a substrate of the enzyme.<sup>17</sup> This molecule hydrogen bonds to Tyr48 and His110 with the phosphate group (with a docking score of  $-38.6$  kcal/mol). This binding mode is in agreement with the crystal structure of the complex between ALR2 and glucose-6-phosphate previously reported,<sup>17</sup> even though the NCI database contained the structure of the open, aldehyde form of glucose-6-phosphate, while the form co-crystallized with ALR2 was the closed one.

We also found several nitro-derivatives interacting with Tyr48 and His110. Phenylsulphonylnitromethane derivatives have in fact been previously reported as ARIs,<sup>27,28</sup> and the crystal structure of the complex between ALR2 and (4-amino-2,6-dimethylphenylsul-

phenyl)nitromethane has also been solved.<sup>21</sup> In the crystal structure, the nitro group of the inhibitor hydrogen bonds to Tyr48 and His110, in full agreement with the docking results of the new nitro-derivatives, which display a similar orientation of the nitro group. Indeed, the NCI database did not contain any sulphonylnitromethane structure, so that this particular class of nitro derivatives could not be retrieved (at least for the sake of validation of the procedure). However, phenylsulphonylnitromethane has an acidity constant of 5.69,<sup>29</sup> and is completely dissociated at physiological pH. For this reason, this particular class of nitro-derivatives might suffer the same disadvantages previously discussed for carboxylic acids. In contrast, all the nitro derivatives in our hit list are neutral at physiological pH, and have a nitro group directly attached to an aromatic system, two conditions that guarantee sufficient diversity from phenylsulphonylnitromethanes.

Finally, docking also selected some 4*H*-1-benzopyran-4-one derivatives within the first 1270 high scoring compounds, among which we found Quercetin, a known inhibitor of ALR2.<sup>30</sup> However, since these compounds are already known as ARIs (see refs 1, 2 and 4, and references therein), we did not include them in the list of the candidates for the biological evaluation. Rather, the attention was focused on carbonyl compounds that differ substantially from 4*H*-1-benzopyran-4-one and, to our knowledge, have not been tested before.

An interesting article by Iwata et al. on the docking of the ACD database into the crystal structure of the ALR2–glucose-6-phosphate complex appeared after our study was completed.<sup>31</sup> Out of 36 best-scoring compounds selected and tested for ALR2 inhibition, ten were classified as active. While Iwata et al. focused their attention on carboxylic acid ARIs and chose to develop indomethacin as a starting lead compound, we preferred to concentrate on new chemical families of ARIs resulting from docking. Moreover, our choice to perform docking on the ALR2 structure with the open, additional hydrophobic pocket observed for Zopolrestat led to hit compounds able to bind the ‘specificity’ pocket, unlike what was reported by Iwata et al., who used an ALR2 structure in which the pocket is closed.

As a matter of fact, a feature common to many of our highest scoring compounds is that they have aromatic substituents inserted into the additional hydrophobic pocket of the enzyme. These substituents vary in shape and complexity, but they all interact with Trp111 and Leu300. This finding is consistent with the binding of the benzothiazole ring of Zopolrestat into the additional hydrophobic pocket, as inferred from X-ray crystallography.<sup>16</sup> Finally, they possess a linker of variable nature which connects the two aromatic fragments of the molecules and allows concomitant occupancy of the active site and the additional hydrophobic pocket.

Then, to reduce the compounds to be tested to a manageable number, a selection of 25 candidates was made after clustering and visual inspection of the complexes. Within each family, the candidates displayed the highest

scores and satisfied the ‘minimal’ requisites for inhibition, that is the formation of hydrogen bonds with Tyr48 and His110, and the presence of a hydrophobic-aromatic fragment inserted into the additional hydrophobic pocket. Their structures, docking scores and inhibitory activities are reported in Table 1. Sorbinil and Tolrestat are included in Table 1 for comparative purposes.

Five carboxylic acid compounds were tested (compounds 1–5 in Table 1, with docking scores ranging from –35.7 to –42.2 kcal/mol). Even though many carboxylic acids are known as ARIs, we wanted to see whether carboxylic acids smaller and simpler than Zopolrestat were still active as ALR2 inhibitors. These low molecular weight compounds proved to be poorly active, compound 2 being the only one with an IC<sub>50</sub> in the micromolar range (28 μM, Table 1). Despite this, all derivatives were predicted to bind in an orientation that had the carboxylate group close to Tyr48 and His110 and an aromatic side chain close to Trp111 and Leu300, in general agreement with the binding mode observed for the tight-binding inhibitor Zopolrestat.<sup>16</sup> However, major differences could be observed: firstly, compounds 1–5, being relatively small, make far fewer hydrophobic contacts with the active site than Zopolrestat;<sup>16</sup> secondly, their conformation is relatively less flexible than Zopolrestat, with the sole exception of the most active compound 2, so that an efficient binding to the Tyr48/His110 active site concomitant with binding to the Trp111/Leu300 hydrophobic pocket might not be as good as in Zopolrestat. At variance with Zopolrestat, in fact, the linker which connects the two aromatic portions of compounds 1, 3 and 5 is less flexible than the methylene linker of Zopolrestat, and the carboxylic acid groups are directly attached to an aromatic ring instead of being separated by a methylene. Compound 4, on the other hand, appears to be too hydrophilic to interact with ALR2 and might suffer a high desolvation penalty. In the structure of the complex between 2 and ALR2, reported in Figure 1, the carboxylate hydrogen bonds to Tyr48, His110 and Trp111 in a way that closely resembles the carboxylate of Zopolrestat (distances to the oxygen of Tyr48 and to the nitrogen of His110 are 2.7 and 2.8 Å, respectively), and the naphthyl ring stacks against Trp111 like the benzothiazole of Zopolrestat. Unlike Zopolrestat, however, 2 cannot form aromatic–aromatic interactions with Trp20, a tryptophan that mutagenesis suggests is very important for tight-binding inhibitors.<sup>32</sup> In agreement with previous evidence that compounds that interact with the additional hydrophobic pocket (the so-called ‘specificity pocket’)<sup>19</sup> are selective for ALR2, compound 2 showed very weak inhibition of ALR1 (6% inhibition at 45 μM, Table 1).

Another family of inhibitors that emerged from the analysis is that of the sulfonic acids (compounds 6–8 in Table 1, docking scores ranging from –40.8 to –47.0 kcal/mol). Compounds 7 and 8 show good inhibitory activity towards ALR2, with IC<sub>50</sub> of 16 and 0.58 μM, respectively. Moreover, they are selective with respect to ALR1 (Table 1). It is predicted that they interact with ALR2 through a dissociated sulfonic acid

**Table 1.** Structures, docking scores (kcal/mol) and inhibitory activities towards ALR2 and ALR1 of the compounds selected after docking

Compd		Docking scores (Kcal/mol)	ALR2 <sup>a</sup>	ALR1 <sup>a</sup>
<i>Carboxylic acids</i>				
1		−40.3	8% inhib at 157 μM	N.T. <sup>b</sup>
2		−42.2	IC <sub>50</sub> 28 μM (23–34)	6% inhib at 45 μM
3		−39.7	27% inhib at 214 μM	N.T.
4		−40.9	0% inhib at 190 μM	N.T.
5		−35.7	6% inhib at 155 μM	N.T.
<i>Sulfonic acids</i>				
6		−40.8	42% inhib at 52 μM	N.T.
7		−47.0	IC <sub>50</sub> 16 μM (12–21)	24% inhib at 26 μM
8		−42.4	IC <sub>50</sub> 0.58 μM (0.49–0.68)	13% inhib at 27 μM
<i>Nitro derivatives</i>				
9		−43.5	30% inhib at 131 μM	N.T.
10		−32.8	18% inhib at 53 μM	N.T.
11		−45.1	4% inhib at 44 μM	N.T.

(continued on next page)

Table 1 (continued)

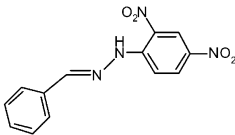
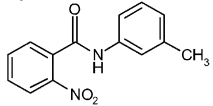
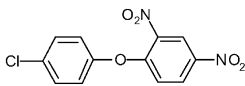
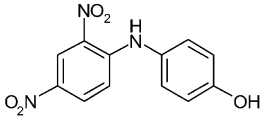
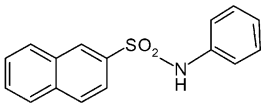
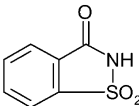
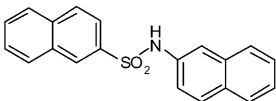
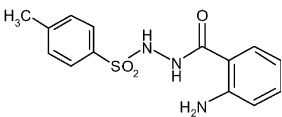
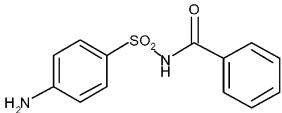
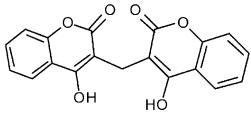
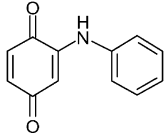
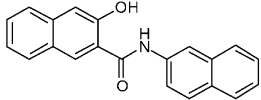
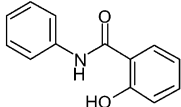
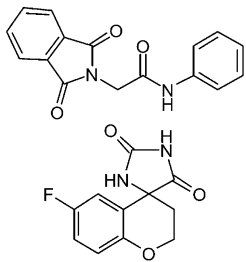
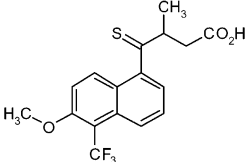
Compd		Docking scores (Kcal/mol)	ALR2 <sup>a</sup>	ALR1 <sup>a</sup>
12		−42.2	0% inhib at 100 μM	N.T.
13		−33.8	12% inhib at 167 μM	N.T.
14		−39.7	9% inhib at 163 μM	N.T.
15		−37.4	IC <sub>50</sub> 42 μM (35–51)	6% inhib at 45 μM
<i>Sulfonamides</i>				
16		−36.9	3% inhib at 40 μM	N.T.
17		−27.3	15% inhib at 227 μM	N.T.
18		−47.7	0% inhib at 25 μM	N.T.
19		−36.9	7% inhib at 146 μM	N.T.
20		−39.7	7% inhib at 143 μM	N.T.
<i>Carbonyl derivatives</i>				
21		−40.7	IC <sub>50</sub> 3.6 μM (2.8–4.6)	21% inhib at 38 μM
22		−31.1	See text	N.T.
23		−38.0	6% inhib at 27 μM	N.T.
24		−33.3	19% inhib at 195 μM	N.T.

Table 1 (continued)

Compd	Docking scores (Kcal/mol)	ALR2 <sup>a</sup>	ALR1 <sup>a</sup>
25	–33.8	5% inhib at 43 $\mu$ M	N.T.
Sorbinil		IC <sub>50</sub> 1.4 $\mu$ M (1.3–1.6)	IC <sub>50</sub> 1.7 $\mu$ M (1.7–1.8)
Tolrestat		IC <sub>50</sub> 0.10 $\mu$ M (0.08–0.12)	IC <sub>50</sub> 1.2 $\mu$ M (0.9–1.7)

<sup>a</sup>IC<sub>50</sub> values ( $\mu$ M) (95% confidence limits) or % inhibition at a given concentration.

<sup>b</sup>N.T., not tested (inhibitory activities toward ALR1 were determined only for the compounds that sensitively inhibit ALR2).

group, which establishes strong hydrogen bonds with Tyr48 and His110 (Fig. 1). It is predicted that compound **7** interacts with Tyr48 and His110 via the sulfonic acid at position 1, and compound **8** via the sulfonic acid at position 2. In addition, they both bind the hydrophobic pocket of the enzyme, compound **7** with the naphthyl ring and compound **8** with the *m*-xylene ring. Given the structures of the complexes (Fig. 1), compound **7** interacts with ALR2 less efficiently than **8**: the naphthalene ring bearing the two sulfonic acid substituents of **7** is almost perpendicular to Trp20, a far from ideal orientation for stacking interactions, while the corresponding naphthalene ring of **8** is almost parallel to Trp20. Compound **6**, which is not as active as **7** and **8**, has two chlorine atoms on the terminal phenyl ring that, given the structure of the complex, might not be the best substituents for a suitable interaction with ALR2. Removal of the two methyl groups of the phenyl ring of **8**, with particular emphasis on the methyl group in *para* which is close to the hydrophilic Thr113 side chain, would probably enhance inhibitory activity.

A major drawback of these new inhibitors is that sulfonic acids are completely dissociated at physiological pH and might suffer the same disadvantages observed for carboxylic acid inhibitors, that is they might show poor activity *in vivo*.

Of the nitro derivatives emerging from docking, compounds **9–15** in Table 1 (docking scores from –32.8 to –45.1 kcal/mol) were selected and tested for ALR2 inhibition. Most of them exhibited modest or even zero inhibitory activity at the maximum concentration they were tested, with the sole exception of compound **15**, which inhibits ALR2 with an IC<sub>50</sub> of 42  $\mu$ M. In general, all nitro-derivatives hydrogen bond to Tyr48 and His110 through the nitro function (which thus acts as a structural replacement for carboxylates). Some of them even possess two nitro-groups (**12**, **14** and **15**), but only

one of them is predicted to interact at the anion binding site and so to be important for inhibitory activity. In addition, they all present an aromatic side chain inserted in the additional hydrophobic pocket. Figure 1 reports the structure of the complex between the inhibitor **15** and ALR2. In the complex, the inhibitor hydrogen bonds Tyr48 and His110 with the nitro group at position 2, and the phenol ring is inserted in the additional pocket. The hydroxyl group, in particular, hydrogen bonds to Thr113, a residue previously shown to be of relevance for the binding of benzopyran-4-one inhibitors of ALR2.<sup>33</sup> Compound **14**, which is similar to **15** but has a chlorine substituent instead of a hydroxyl, and an oxygen linker instead of an amino, is significantly less active than **15**.

One of the main reasons why the nitro derivative **15** can be considered an interesting inhibitor is that it has a very simple structure and, unlike phenylsulphonyl-nitromethanes and carboxylic and sulfonic acids, it does not undergo ionisation at physiological pH. The pK<sub>a</sub> prediction of **15**, made with the ACD/pK<sub>a</sub><sup>34</sup> software, is 9.9.

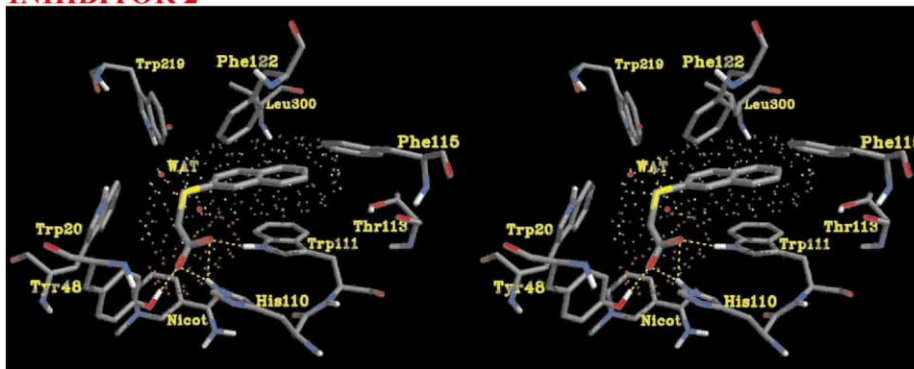
We therefore decided to undertake a round of optimization with the synthesis and biological evaluation of a small series of new derivatives of **15** specially designed to test the binding mode proposed by DOCK and to improve inhibitory activity. Six derivatives of **15**, **15a–15f** in Table 2, were synthesized and tested.

Firstly, the amino linker that bridges the two aromatic rings of **15** was changed to sulfur (**15a**). In the structure of the complex between ALR2 and **15**, in fact, the amino linker that connects the two aromatic rings does not hydrogen bond to any protein residues—rather, it is in contact with hydrophobic residues (Fig. 1). A sulfur bridge was therefore appropriate to increase interaction with ALR2. We found that **15a** is about 6 times more

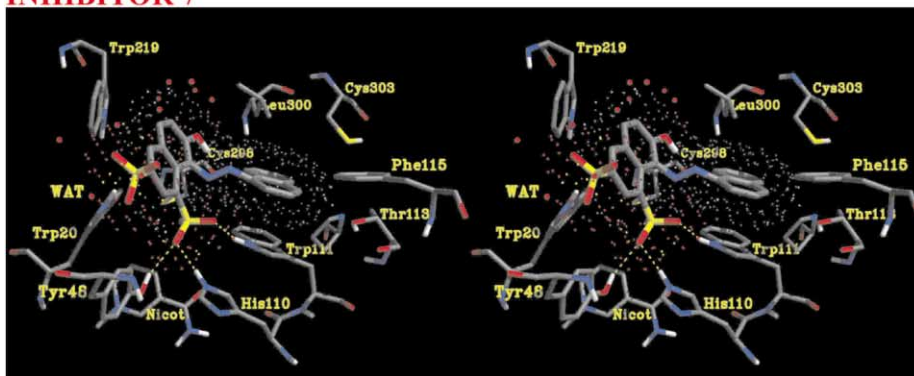
active than **15**, having an  $IC_{50}$  of  $7.4 \mu M$  (Table 2). We therefore decided to maintain the sulfur bridge and to introduce further changes to **15**. To support the prediction that the nitro group at position 2 is much more important than the nitro group at position 4 (since it is the one hydrogen bonded to Tyr48 and His110 in the complex), the two mono-nitro derivatives **15b** and **15c** were synthesized and tested. The inhibitory activity of **15b**, which has the nitro group in position 2, further improves to  $4.8 \mu M$ , while the inhibitory activity of **15c**, with the nitro group in 4, is significantly worse ( $IC_{50}$  is  $30 \mu M$ ). Taken together, these data clearly confirm that the nitro group of **15** most important for binding is the one in position 2, in agreement with the predictions.

The last changes to **15** made it possible to investigate the importance of the 4'-hydroxyl in the interaction with ALR2. In the structure of the complex, this hydroxyl hydrogen bonds Thr113, and so it might contribute favourably to inhibitory activity. Accordingly, the three derivatives **15d**, **15e** and **15f**, which are the non-hydroxylated analogues of **15a**, **15b** and **15c**, respectively, were synthesized and tested. As expected, a systematic reduction in inhibitory activity was observed for the non-hydroxylated compounds (Table 2). Comparison of **15e** with **15f** confirms that the 2-nitro substituent is, again, the most important for inhibition, **15e** having an  $IC_{50}$  of  $22 \mu M$  while **15f** displays no inhibition up to  $48 \mu M$  concentration. Finally, all the nitro derivatives in

## INHIBITOR 2



## INHIBITOR 7



## INHIBITOR 8

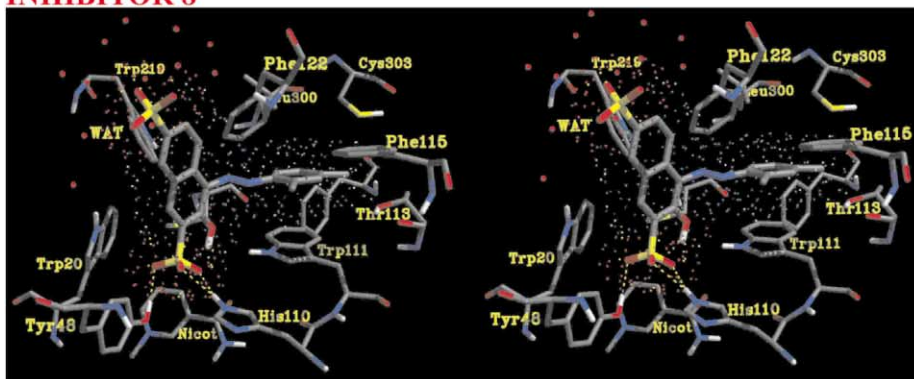


**Figure 1.** Stereoviews of active site residues of ALR2 interacting with the inhibitors **2**, **7**, **8**, **15** and **21** after refinement with MD. Stereoviews showing compounds **16** and **20** bound to ALR2 are also shown, as their orientation significantly differs from the orientation found by DOCK (shown as white thin bonds, for comparison). For clarity, only the polar hydrogens are shown. Inhibitors are highlighted with their van der Waals surfaces, and hydrogen bonds are shown as dotted lines. Water molecules are shown as dots (*continued on next page*).



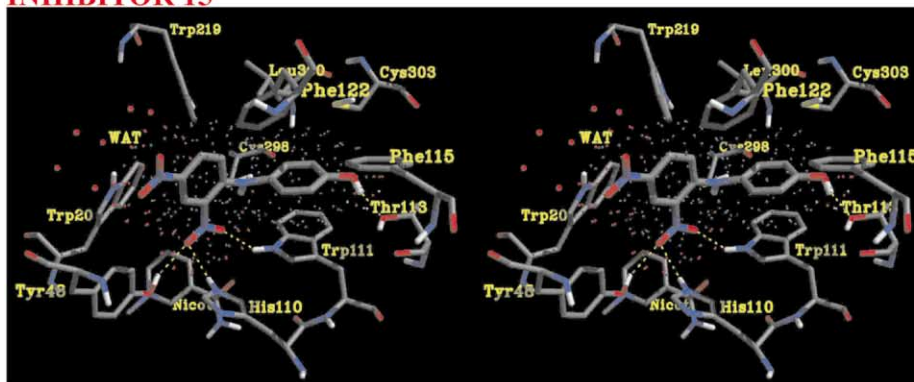
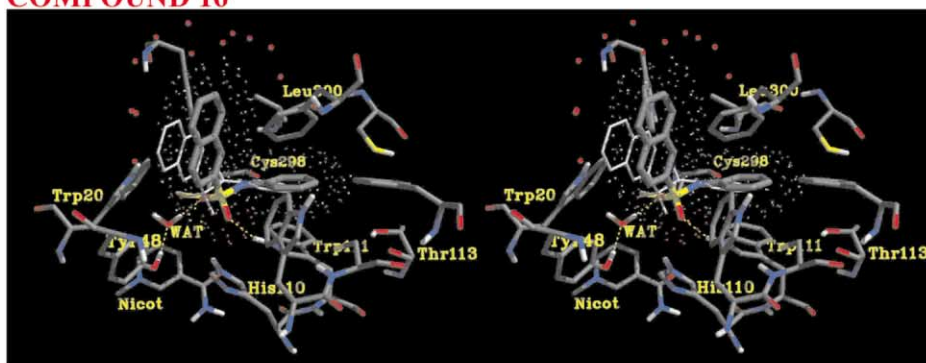
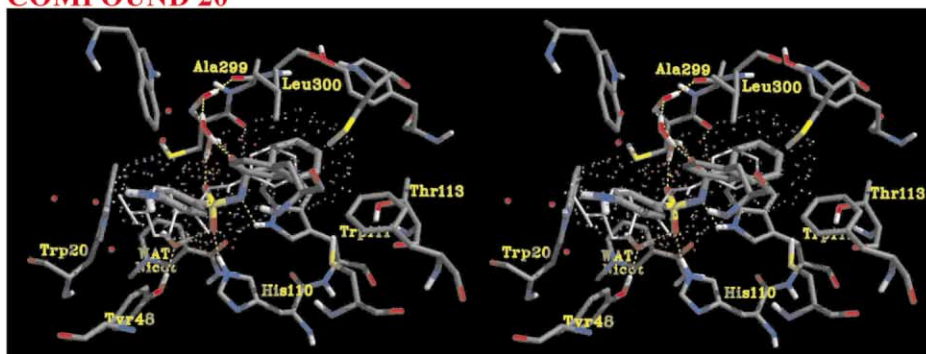
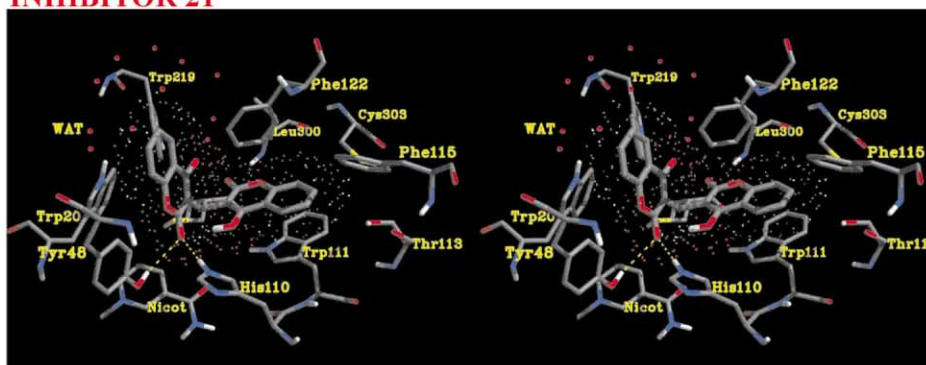
**INHIBITOR 15****COMPOUND 16****COMPOUND 20****INHIBITOR 21**

Figure 1. (continued)

Table 2 are selective for ALR2: the most active compound in the series, **15b**, shows a 10-fold selectivity for ALR2 with respect to ALR1 (Table 2).

The sulfonamide derivatives **16–20** in Table 1 (docking scores from  $-27.3$  to  $-47.7$  kcal/mol) are not active. It was predicted that they would hydrogen bond to Tyr48 and His110 via the sulfone group, which appeared to be an interesting replacement for the carboxylate groups of inhibitors like Tolrestat and Zopolrestat. ALR2 inhibitors carrying a sulfonamide group were previously reported for a series of *N*-(phenylsulfonyl)glycines,<sup>35,36</sup> but these derivatives likely owe their activity to the carboxylate group of the glycine rather than to the sulfonamide. On the contrary, derivatives **16–20** do not have any carboxylate, and the recognition pharmacophore is the sulfonamide.

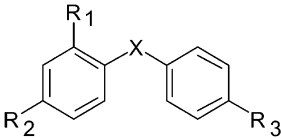
To predict whether the sulfonamide nitrogens can or cannot undergo dissociation at physiological pH, a prediction of the acidity constants ( $pK_a$ ) of **16–20** was made with the use of ACD/ $pK_a$ .<sup>34</sup> Two types of sulfonamides were identified depending on the protonation state of the sulfonamide: it was predicted that compounds **16** and **18**, in which a sulfonamide connects two aromatic rings, would be neutral at physiological pH (predicted  $pK_a$  being 8.5 and 8.3, respectively). On the other hand, it was predicted that compounds **17** and **20**, having a carbonyl adjacent to the sulfonamide, would be much more acidic (predicted  $pK_a$  being 4.5 and 6.7, respectively). This is probably attributable to the delocalization effects of the negative charge of the dissociated sulfonamide to the adjacent carbonyl oxygen, which has partial enolate character. Finally, compound **19** displays intermediate behaviour, having a predicted  $pK_a$  close to the physiological pH (7.4).

To find out why sulfonamides are not active as ALR2 inhibitors, molecular dynamics simulations were performed for the complexes of **16** (neutral molecule at physiological pH) and **20** (anionic molecule at physiological pH). In both cases, we found that a water molecule enters into the active site cleft and hydrogen bonds to Tyr48 (Fig. 1). Thus, hydrogen bonding between the sulfone group and this residue turns out to be mediated by a water molecule bridge. This might be

the reason why the sulfonamides in question have very weak inhibition profiles compared with other inhibitors. The situation presumably arises because the pharmacophore element designed to bind the active site Tyr48 and His110 residues (the sulfone group) is also part of the linker that connects the two aromatic portions of the molecules, so that a concomitant binding to the active site and to the hydrophobic pocket is conformationally constrained. This finding was not predicted by docking, and points to the importance of applying molecular dynamics after docking to permit an efficient sampling of conformational states and to account for induced-fit. Comparison with the orientation found by DOCK shows that compound **20** undergoes conformational changes around the sulfonamide and carbonyl bonds during molecular dynamics (Fig. 1; the docked orientation is shown in white, thin bonds). The water molecule hydrogen bonds to Tyr48 and to one of the sulfone oxygens of **20** which, in turn, hydrogen bonds to His110. The dissociated amide nitrogen hydrogen bonds to Trp111, and three water molecules connect the other sulfone oxygen and the carbonyl of **20** with the backbone of Ala299. As for the orientation of compound **16**, the neutral sulfonamide derivative, the difference between the docked and the MD orientations is similar to **20** (Fig. 1). Again, this is mainly due to the presence of a water molecule hydrogen bonding to Tyr48 and one sulfone oxygen, which displaces the sulfone group far from Tyr48 and, to a lesser extent, His110. Compared with the docking orientation, the naphthalene ring is rotated by  $180^\circ$  in the orientation obtained after MD.

The last class of compounds selected by DOCK presents a carbonyl group hydrogen bonding to both Tyr48 and His110 (compounds **21–25** in Table 1, docking scores ranging from  $-31.1$  to  $-40.7$  kcal/mol). Again, they have an aromatic substituent inserted in the additional hydrophobic pocket. Promising results were obtained for the bis-coumarin derivative **21**, which inhibits ALR2 with an  $IC_{50}$  of  $3.6 \mu\text{M}$  and only marginally inhibits ALR1 (21% inhibition at  $38 \mu\text{M}$ , Table 1). Coumarins were previously reported to inhibit ALR2,<sup>37</sup> but none of the compounds tested so far had a bis-coumarin structure: the reason why this could make the difference is that, in the structure of the ALR2-bis-coumarin complex, one of the coumarin rings can interact with Tyr48

Table 2. Development of the nitro derivative **15**

						
Compd	R <sub>1</sub>	R <sub>2</sub>	R <sub>3</sub>	X	ALR2 <sup>a</sup>	ALR1 <sup>a</sup>
<b>15</b>	NO <sub>2</sub>	NO <sub>2</sub>	OH	NH	42 $\mu\text{M}$ (37–47)	6% inhib at 45 $\mu\text{M}$
<b>15a</b>	NO <sub>2</sub>	NO <sub>2</sub>	OH	S	7.4 $\mu\text{M}$ (5.7–9.5)	31% inhib at 43 $\mu\text{M}$
<b>15b</b>	NO <sub>2</sub>	H	OH	S	4.8 $\mu\text{M}$ (4.0–5.8)	48 $\mu\text{M}$ (41–56)
<b>15c</b>	H	NO <sub>2</sub>	OH	S	30 $\mu\text{M}$ (23–40)	39% inhib at 57 $\mu\text{M}$
<b>15d</b>	NO <sub>2</sub>	NO <sub>2</sub>	H	S	19% inhib at 32 $\mu\text{M}$	0% inhib at 47 $\mu\text{M}$
<b>15e</b>	NO <sub>2</sub>	H	H	S	22 $\mu\text{M}$ (18–27)	8% inhib at 59 $\mu\text{M}$
<b>15f</b>	H	NO <sub>2</sub>	H	S	0% inhib at 48 $\mu\text{M}$	0% inhib at 61 $\mu\text{M}$

<sup>a</sup>See footnotes to Table 1.

and His110, and the other can bind the additional hydrophobic pocket lined by Trp111, Leu300 and Phe122, providing specificity for ALR2 compared to ALR1. 4-hydroxycoumarins, as in the case of molecule **21**, have acidity constants comparable with those of carboxylic acids (the experimental  $pK_a$  of 4-hydroxycoumarin is 5.1).<sup>38</sup> The prediction of the  $pK_a$  of **21**, made with ACD/ $pK_a$ ,<sup>34</sup> gave two dissociation constants, the first corresponding to dissociation of the first 4-hydroxyl with a  $pK_a$  of 4.2, and the second corresponding to dissociation of the second 4-hydroxyl (thus producing a dianionic form) with a  $pK_a$  of 8.6. Given these predictions, the bis-coumarin **21** was modeled as a mono-anion, with the dissociated 4-hydroxy coumarin ring inserted in the active site and the neutral 4-hydroxy coumarin ring inserted in the hydrophobic pocket. In the structure of the complex (Fig. 1), the 2-carbonyl of **21** hydrogen bonds to Tyr48 and His110, while the dissociated 4-hydroxyl is exposed to solvent. The neutral coumarin ring is inserted in the hydrophobic pocket and interacts with Trp111, Leu300 and Phe122.

The quinone derivative **22** is predicted to bind the anionic site of ALR2 via a carbonyl group hydrogen bonded to Tyr48 and His110, and the additional pocket via its 2-phenyl ring. Literature data are in agreement with these results: Menadione, a quinone derivative possessing ALR2 inhibitory activity, was found to be able to form a non-covalent complex with ALR2 prior to formation of a covalent bond with Cys298.<sup>39</sup> However, the inhibitory activity of **22** could not be assessed in our study, since dithiotreitol (DTT) is present in the assay solution and quinones are known to react with thiols.<sup>39</sup>

### Conclusions

We have presented a structure-based design of new inhibitors of aldose reductase. Using the DOCK program, the NCI database of compounds was searched for molecules complementary to the ALR2 active site. This search led to the discovery of five novel compounds that inhibited ALR2 in the micromolar range and showed selectivity with respect to ALR1. Remarkably, these compounds do not belong to the classes of the carboxylic acid or spirohydantoin, which have long been studied and optimized as ARIs. A class of particularly interesting nitro-derivatives with sufficient diversity from existing inhibitors was identified and exploited with a round of optimization through structure-based design and synthesis. Starting from the bioactive compound having an  $IC_{50}$  of 42  $\mu$ M, we succeeded in obtaining a derivative with a 10-fold improved  $IC_{50}$  and 10-fold selectivity with respect to ALR1. Structure-activity relationships within the series of the nitro derivatives were in agreement with the binding mode at the active site.

Overall, our results further demonstrate the effectiveness of docking and structure-based drug design for the de-novo discovery of inhibitors and their subsequent optimization. In this context, refinement of enzyme-

inhibitor complexes with molecular dynamics and inclusion of solvent effects turn out to be important aspects of the design.

## Experimental

### Docking

The aldose reductase structure used for docking is the one previously obtained by docking and energy minimization of a complex between ALR2 and a carboxylic acid inhibitor carrying a benzothiazole substituent.<sup>22</sup>

Docking of inhibitors was performed using the program DOCK 3.5,<sup>40</sup> which consists of several modules. The module SPHGEN<sup>41</sup> was used to generate clusters of overlapping spheres that describe the accessible surface of the active site. Seventy four spheres were used to describe the active site of the enzyme. The module CHEMGRID<sup>42</sup> was then used to precompute and save in a grid file the information necessary for force-field scoring. This scoring function approximates molecular mechanics interaction energies and consists of van der Waals and electrostatic components.<sup>42</sup>

As regards the database of organic molecules, we used the National Cancer Institute (NCI-3-D) database (available on the network at the address <http://dtp.nci.nih.gov>). It includes the 3-D structures of more than 127,000 organic molecules. For convenience, the database was divided into smaller subsets of 10,000 molecules each, which were processed independently. In order to be used by DOCK, Sybyl atom types were automatically assigned using the sdf2mol2 utility, and the protonation state of charged functional groups such as carboxylates, guanidinium ions and so on, was properly assessed. Then, the Sybyl program was used to add hydrogens to the molecules and to assign partial charges to atoms according to Gasteiger-Marsili.

The program DOCK3.5 was then run to find and score orientations of each molecule of the database in the active site of ALR2. Each orientation was filtered for steric fit with a DISTMAP grid<sup>43</sup> with polar and non-polar contact limits of 2.3 and 2.8 Å, respectively. Orientations that passed this steric filter were evaluated for van der Waals and electrostatic complementarity using the grids calculated by CHEMGRID. On average, the docking of each compound in the database required 4 s of CPU time on a SGI-R5000 computer.

For each reduced subset of the database (10,000 compounds), the first 100 highest scoring compounds were saved. Their complexes with ALR2 were visually inspected using the computer graphics program MidasPlus.<sup>44</sup> The hit compounds (1270) were clustered into chemical families according to the functional group interacting with Tyr48 and His110. From the 1270 hits, 25 candidates were finally selected. For the molecules that were not commercially available, we searched the chemical catalogs for very similar compounds, using ChemFinder 4.0.<sup>45</sup> In this stage, we made sure that

changes introduced into the original structures did not alter their ability to bind the key residues of the active site. The modified hits were re-docked into the binding site of ALR2, to ensure that the changes in structure did not significantly affect the orientation and the score.

### Purchase of molecules

Molecules were purchased from Sigma-Aldrich, with the sole exception of compound **25**, which was synthesized according to ref 46. Referring to Table 1, compounds are: (1) 2'-carboxy-2-hydroxy-4-methoxybenzophenone; (2) (2-naphthylthio)acetic acid; (3) *N*-phenylanthranilic acid; (4) *N*-benzoyl-L-threonine; (5) 2-(1-naphthoyl)-benzoic acid; (6) 2-amino-6-chloro-3-(2,4-dichlorophenoxy)benzenesulfonic acid; (7) Crystal Ponceau 6R; (8) Xylidine Ponceau 2R; (9) 1-nitro-2-*p*-toluen sulfonamido naphthalene; (10)  $\alpha$ -(2-methoxy-5-nitrophenylimino)-*o*-cresol; (11) 3-((2-nitro-phenyl)hydrazono)-1,3-dihydro-indol-2-one; (12) benzaldehyde-(2,4-dinitrophenyl)hydrazone; (13) 2-nitrobenzo-*m*-toluidide; (14) 4'-chloro-2,4-dinitrophenylether; (15) 4-(2,4-dinitroanilino)phenol; (16) naphthalene-2-sulfonic acid phenylamide; (17) saccharin; (18) naphthalene-2-sulfonic acid naphthalen-2-yl-amide; (19) 1-anthraniloyl-2-(*p*-tolylsulfonyl)hydrazine; (20) sulfabenzamide; (21) 3,3'-methylenebis-4-hydroxycoumarin; (22) 2-phenylamino-1,4-benzoquinone; (23) 3-hydroxynaphthalene-2-carboxylic acid naphthalen-2-yl-amide; (24) salicylanilide; (25) 2-(1,3-dioxo-1,3-dihydroisindol-2-yl)-*N*-phenyl acetamide.

### Molecular mechanics

The structures of the complexes between ALR2 and the inhibitors here discovered were energy-minimized with the AMBER 5<sup>47</sup> program using the Cornell et al.<sup>48</sup> force field. To calculate the partial atomic charges of inhibitors that were consistent with the AMBER force field, the geometries of the molecules were completely optimized using the AM1Hamiltonian, and charges were calculated with electrostatic potential fits to a 6-31G\* ab-initio wave function using Gaussian98, followed by a standard RESP<sup>49,50</sup> fit. Van der Waals parameters of the inhibitors were assigned to be consistent with the Cornell force field. Parameters for NADP<sup>+</sup> were taken from our previous simulations.<sup>22,51</sup> Dihedral parameters consistent with the Cornell et al. parameterization were assigned and, in some cases, derived from a conformational analysis performed with AM1. For each molecule, energy minimization was performed to make sure that the optimized conformation was in agreement with the AM1-optimized conformation.

The ALR2-inhibitor complexes resulting from DOCK were solvated with spherical caps of TIP3P<sup>52</sup> water molecules within 24 Å of the inhibitors. The number of water molecules ranged between 410 and 520, depending on the size of the inhibitor. Harmonic radial forces (1.5 kcal/mol Å<sup>2</sup>) were applied to avoid evaporation.

Prior to energy-minimization of the complexes, only the water molecules were energy-minimized and then sub-

jected to 20 ps of molecular dynamics at 300 K, in order to let the solvent equilibrate around the enzyme-inhibitor structure. Then, 5000 steps of conjugate gradient minimization were performed, with all protein residues within 10 Å from the inhibitor and all the water molecules allowed to move during minimization. A 10 Å non-bonded cutoff was adopted in the simulations. Molecular dynamics was then performed on the ALR2-inhibitor complexes at 300 K for over 400 ps. The complexes were gradually heated to 300 K during the first 20 ps, in order to avoid abrupt changes of structure. SHAKE<sup>53</sup> was turned on during molecular dynamics and a time-step of 2.0 fs was used. Coordinates were collected every 0.2 ps, and averaged with CARNAL every 10 ps. Finally, the last averaged structure resulting from molecular dynamics was re-optimized with 5000 steps of conjugate gradient minimization.

Molecular dynamics calculations were performed on a IBM-SP3 computer, and graphic display was performed on SGI O2 workstations.

### Synthesis

The compounds **15a–f** were obtained from the reaction between 2- or 4-bromonitrobenzene and the appropriate thiophenol in alkaline medium.

Melting points were determined on a Buchi 510 capillary melting point apparatus and are uncorrected. Elemental analysis for compound **15a** was conducted in the Microanalysis laboratory of the Dipartimento di Scienze Farmaceutiche, Modena University, and was within  $\pm 0.4\%$  of the theoretical values. <sup>1</sup>H NMR spectra were recorded on a Bruker AC200 spectrometer; chemical shifts are reported as  $\delta$  (ppm) relative to tetramethylsilane as internal standard. DMSO-*d*<sub>6</sub> was used as solvent.

A solution of 4-hydroxythiophenol (for compounds **15a–c**) or a solution of thiophenol (for **15d–f**) (5.63 mmols) in EtOH (2 mL) was added to a solution of the appropriate bromonitrobenzene (5.0 mmols) in EtOH (10 mL), then K<sub>2</sub>CO<sub>3</sub> (for **15a–c**, 5.63 mmols) or pulverized KOH (for **15d–f**) (5.63 mmols) was added. The suspension was warmed at 70 °C for 15 h, cooled, then water was added. For compounds **15a–c** the pH of the solution was adjusted to pH 5.00, then the solution was extracted with EtOAc (3×30 mL). The organic layer was washed (for compounds **15d–f**) with KOH 2N (2×20 mL), then the organic layer was dried (Na<sub>2</sub>SO<sub>4</sub>) and evaporated to dryness under reduced pressure. The residue was purified as described.

**4-(2,4-Dinitrophenylmercapto)phenol (15a).** Yield 85%, mp 159–160 °C (MeOH/H<sub>2</sub>O). <sup>1</sup>H NMR: 10.25 (1H, s), 8.90 (1H, d, *J* = 2.50), 8.37 (1H, dd, *J* = 2.50, *J* = 8.00), 7.48 (2H, m), 7.03 (3H, m). C<sub>12</sub>H<sub>8</sub>N<sub>2</sub>O<sub>5</sub>S: C, H, N.

**4-(2-Nitrophenylmercapto)phenol (15b).** Yield 68%, mp 133–134 °C (MeOH/H<sub>2</sub>O) (130–132 °C).<sup>54</sup> <sup>1</sup>H NMR: 10.16 (1H, s), 8.24 (1H, dd, *J* = 1.40, *J* = 8.20), 7.58 (1H, m), 7.39 (3H, m), 6.95 (2H, m), 6.83 (1H, dd, *J* = 1.20, *J* = 9.30).

**4-(4-Nitrophenylmercapto)phenol (15c).** Yield 68%, mp 143–145 °C (MeOH/H<sub>2</sub>O) (150 °C).<sup>55</sup> <sup>1</sup>H NMR: 10.15 (1H, s), 8.13 (2H, m), 7.44 (2H, m), 7.18 (2H, m), 6.94 (2H, m).

**(2,4-Dinitrophenyl)phenylsulfide (15d).** Yield 77%, mp 118–120 °C (EtOH) (120–121 °C).<sup>56</sup> <sup>1</sup>H NMR: 8.90 (1H, d, *J* = 2.00), 8.35 (1H, dd, *J* = 2.50, *J* = 8.35), 7.68 (5H, m), 7.05 (1H, d, *J* = 8.00).

**(2-Nitrophenyl)phenylsulfide (15e).** Yield 79%, mp 80–82 °C (EtOH) (78–80 °C).<sup>57</sup> <sup>1</sup>H NMR: 8.22 (1H, dd, *J* = 1.28, *J* = 8.23), 7.66 (6H, m), 7.40 (1H, m), 6.87 (1H, dd, *J* = 1.28, *J* = 8.23).

**(4-Nitrophenyl)phenylsulfide (15f).** Yield 79%, mp 52–53 °C (EtOH) (55 °C).<sup>58</sup> <sup>1</sup>H NMR: 8.13 (2H, m), 7.56 (5H, m), 7.27 (2H, m).

Tolrestat was synthesized according to a procedure reported in the literature.<sup>59</sup> Sorbinil was a gift from Pfizer (Groton, CT, USA).

### Enzyme section

Partially purified ALR2 was used for the inhibitory assays. Calf lenses were obtained locally from freshly-slaughtered animals. The capsule was incized, and the frozen lenses were suspended in 10 mM sodium phosphate buffer pH 7.00 containing 5 mM DTT (1 g tissue/3.5 mL) and stirred in an ice cold bath for 1 h. The suspension was then centrifuged at 22,000g at 4 °C for 40 min, and ALR2 present in the supernatant was partially purified by ion exchange chromatography on DE52, as previously described.<sup>51</sup> Enzyme activity was measured by monitoring the change in absorbance at 340 nm which accompanies the oxidation of NADPH catalyzed by ALR2. The assays were performed as previously described,<sup>51</sup> using 4.7 mM D,L-glyceraldehyde as substrate in 0.25 M sodium phosphate buffer, pH 6.80, containing 0.38 M ammonium sulfate and 0.11 mM NADPH (37 °C).

Partially-purified ALR1 used in the inhibitory assays was obtained following a previously reported method.<sup>51</sup> Bovine kidneys were homogenized in 3 vol of 0.25 M sucrose, 2.0 mM EDTA dipotassium salt and 2.5 mM β-mercaptoethanol in 10 mM sodium phosphate buffer, pH 7.2 (S-Buffer). The homogenate was centrifuged (16,000g for 20 min at 4 °C) and the supernatant subjected to ammonium sulfate fractional precipitation. The pellet obtained between 45 and 75% of salt saturation, containing ALR1 activity, was redissolved in S-buffer containing 2.0 mM EDTA (dipotassium salt) and 2.0 mM β-mercaptoethanol at a protein concentration of approximately 20 mg/mL. DEAE-52 resin was added to the solution and then removed by centrifugation. The enzyme preparation appeared devoid of any ALR2 activity, being ineffective in reducing glucose (up to 150 mM D-glucose used as substrate) and displaying an IC<sub>50</sub> for valproate of 2.01 (1.37–2.93) μM. ALR1 activity was assayed at 37 °C using 20 mM D-glucuronate as substrate and 0.12 mM NADPH in 0.1 M sodium phosphate buffer, pH 7.2.

The sensitivity of the enzymes to inhibition by the compounds under study was tested in the above assay conditions by including the inhibitor dissolved in DMSO at the desired concentrations in the reaction mixture. DMSO in the assay mixture was kept at a constant concentration of 1%. A reference blank containing all the above reagents except the substrate was used to correct for the nonenzymatic oxidation of NADPH. Compounds were tested at the highest concentration allowed before precipitation in the enzymatic assay solution. When 50% inhibition of the enzymatic reaction could not be observed at this concentration, the % inhibition at the maximum solubility concentration of each compound was reported. IC<sub>50</sub> values (the concentration of the inhibitor required to produce 50% inhibition of the enzyme catalysed reaction) were determined from least-squares analyses of the linear portion of the log dose-inhibition curves. Each curve was generated using at least three concentrations of inhibitor causing an inhibition between 20 and 80%, with two replicates at each concentration. The 95% confidence limits (95% CL) were calculated from *T* values for *n*–2, where *n* is the total number of determinations.<sup>60</sup> Sorbinil and Tolrestat were used as controls.

### Elemental analyses

Compound	Formula	C Calcd/ found	H Calcd/ found	N Calcd/ found
<b>15a</b>	C <sub>12</sub> H <sub>8</sub> N <sub>2</sub> O <sub>5</sub> S	49.32/ 49.65	2.76/ 2.59	9.58/ 9.50

### Acknowledgements

Financial support from Consiglio Nazionale delle Ricerche (grant CNR no. 98.01911.CT03) is gratefully acknowledged. Thanks are due to Prof. Stefano Manfredini (University of Ferrara) for allowing us to use Sybyl to convert the NCI-3-D database in a format suitable for DOCK3.5.

### References and Notes

- Kador, P. F. *Med. Res. Rev.* **1988**, *8*, 325.
- Tomlinson, D. R.; Stevens, E. J.; Diemel, L. *Trends Pharm. Sci.* **1994**, *15*, 293.
- Carper, D. A.; Wistow, G.; Nishimura, C. *Exp. Eye Res.* **1989**, *49*, 377.
- Costantino, L.; Rastelli, G.; Cignarella, G.; Vianello, P.; Barlocco, D. *Exp. Opin. Ther. Pat.* **1997**, *7*, 843.
- The Diabetes Control and Complications Trial Research Group. *New Engl. J. Med.* **1993**, *329*, 977.
- Sarges, R. *Adv. Drug Res.* **1989**, *18*, 139.
- Humber, L. G. *Prog. Med. Chem.* **1987**, *24*, 299.
- (a) Eggler, J. F.; Larson, E. R.; Lipinski, C. A.; Mylari, B. L.; Urban, F. J. A Perspective of Aldose Reductase Inhibitors. In *Advances in Medical Chemistry*; Jai: Greenwich, 1993. (b) Humber, L. G. *Prog. Med. Chem.* **1987**, *24*, 299.

9. Kuntz, I.D.; Meng, E.C.; Shoicket, B.K. Challenges in structure-based drug design. In *New Perspectives in Drug Design*, Dean, P. M., Jolles, G., Newton, C. G., Eds.; Academic: London, 1995; p 137.
10. Mason, J. S.; McLay, I. M.; Lewis, R. A. Applications of Computer-aided Drug Design Techniques to Lead Generation. In *New Perspectives in Drug Design*, Dean, P. M., Jolles, G., Newton, C. G., Eds.; Academic: London, 1995; p 225.
11. Balbes, L.M.; Mascarella, S.W.; Boyd, D.B. A Perspective of Modern Methods in Computer-aided Drug Design. In *Reviews in Computational Chemistry*, Lipkowitz, K. B., Boyd, D. B., Eds.; VCH: New York, 1994; Vol. 5, p 337.
12. Borman, S. *Chem. Eng. News* **1992**, 10, 18.
13. Good, A. C.; Mason, S. J. Three dimensional structure database searches. In *Reviews in Computational Chemistry*; Lipkowitz, K. B., Boyd, D. B., Eds.; VCH: New York, 1996; Vol. 7, p 67.
14. Kuntz, I. D.; Meng, E. C.; Shoicket, B. K. *Acc. Chem. Res.* **1994**, 27, 117.
15. Shoicket, B. K.; Perry, K. M.; Santi, D. V.; Stroud, R. M.; Kuntz, I. D. *Science* **1993**, 259, 1445.
16. Wilson, D. K.; Tarle, I.; Petrash, J. M.; Quiocho, F. A. *Proc. Natl. Acad. Sci. U.S.A.* **1993**, 90, 9847.
17. Harrison, D. H.; Bohren, K. M.; Ringe, D.; Petsko, G. A.; Gabbay, K. H. *Biochemistry* **1994**, 33, 2011.
18. Bohren, K. M.; Grimshaw, C. E.; Lai, C. J.; Harrison, D. H.; Ringe, D.; Petsko, G. A.; Gabbay, K. H. *Biochemistry* **1994**, 33, 2021.
19. Urzhumtsev, F.; Tete-Favier, A.; Mitsler, J.; Barbanton, P.; Barth, L.; Urzhumtseva, J. F.; Biellmann, A. D.; Podjarny, D.; Moras, D. A. *Structure* **1997**, 5, 601.
20. Calderone, V.; Chevrier, B.; Van Zandt, M.; Lamour, V.; Howard, E.; Poterszman, A.; Barth, P.; Mitsler, A.; Lu, J.; Dvornik, D. M.; Klebe, G.; Kraemer, O.; Moorman, A. R.; Moras, D.; Podjarny, A. *Acta Cryst. Sect. D* **2000**, D56, 536.
21. Rogniaux, H.; van Dorsselaer, A.; Barth, P.; Biellmann, J. F.; Barbanton, J.; van Zandt, M.; Chevrier, B.; Howard, E.; Mitsler, A.; Potier, N.; Urzhumtseva, L.; Moras, D.; Podjarny, A. *J. Am. Soc. Mass Spectrom.* **1999**, 10, 635.
22. Rastelli, G.; Vianello, P.; Barlocco, D.; Costantino, L.; Del Corso, A.; Mura, U. *Bioorg. Med. Chem. Lett.* **1997**, 7, 1897.
23. Bohm, H. J. *J. Comput.-Aided Mol. Des.* **1998**, 12, 309.
24. Muegge, I.; Martin, Y. C. *J. Med. Chem.* **1999**, 42, 791.
25. Tame, J. R. H. *J. Comput.-Aided Mol. Des.* **1999**, 13, 99.
26. Claußen, H.; Buning, C.; Rarey, M.; Lengauer, T. *J. Mol. Biol.* **2001**, 308, 377.
27. Ward, W. H. J.; Cook, P. N.; Mirrlees, D. J.; Brittain, D. R.; Preston, J.; Carey, F.; Tuffin, D. P.; Howe, R. *Biochem. Pharmacol.* **1991**, 42, 2115.
28. Saab, N. H.; Donkor, I. O.; Rodriguez, L.; Kador, P.; Miller, D. D. *Eur. J. Med. Chem.* **1999**, 34, 745.
29. Bordwell, F. G.; Bartmess, J. E. *J. Org. Chem.* **1978**, 43, 3101.
30. Varma, S. D.; Kinoshita, J. H. *Biochem. Pharmacol.* **1976**, 25, 2505.
31. Iwata, Y.; Arisawa, M.; Hamada, R.; Kita, Y.; Mizutani, M. Y.; Tomioka, N.; Itai, A.; Miyamoto, S. *J. Med. Chem.* **2001**, 44, 1718.
32. Hohman, T. C.; El-Kabbani, O.; Malamas, M. S.; Lai, K.; Putilina, T.; McGowan, M. H.; Wane, Y.-Q.; Carper, D. S. *Eur. J. Biochem.* **1998**, 256, 310.
33. Costantino, L.; Rastelli, G.; Gamberini, M. C.; Vinson, J. A.; Bose, P.; Iannone, A.; Staffieri, M.; Antolini, L.; Del Corso, A.; Mura, U.; Albasini, A. *J. Med. Chem.* **1999**, 42, 1881.
34. The results of ACD/pK<sub>a</sub> version 4.5 were obtained using the ACD/I-Lab Web service (<http://www2.acdlabs.com/ilab/>).
35. DeRuiter, J.; Brubaker, A. N.; Garner, M. A.; Barksdale, J. M.; Mayfield, C. A. *J. Pharm. Sciences* **1987**, 76, 149.
36. DeRuiter, J.; Borne, R. F.; Mayfield, C. A. *J. Med. Chem.* **1989**, 32, 145.
37. Okada, Y.; Miyauchi, N.; Suzuki, K.; Kobayashi, T.; Tsutsui, C.; Mayuzumi, K.; Nishibe, S.; Okuyama, T. *Chem. Pharm. Bull.* **1995**, 43, 1385.
38. Arora, H. K.; Aggarwal, A. R.; Ray, N. K.; Ahluwalia, V. K.; Singh, R. P. *Indian J. Chem.* **1981**, 20A, 168.
39. Bhanagar, A.; Liu, S.I.-QI.; Petrash, J. M.; Srivastava, S. K. *Mol. Pharmacol.* **1992**, 42, 917.
40. Gschwend, D. A.; Kuntz, I. D. *J. Comput. Aided Mol. Des.* **1996**, 10, 123.
41. Kuntz, I. D.; Blaney, J. M.; Oatley, S. J.; Langridge, R.; Ferrin, T. E. *J. Mol. Biol.* **1982**, 161, 269.
42. Meng, E. C.; Shoicket, B. K.; Kuntz, I. D. *J. Comput. Chem.* **1992**, 13, 505.
43. Shoicket, B. K.; Bodian, D. L.; Kuntz, I. D. *J. Comput. Chem.* **1992**, 13, 380.
44. Ferrin, T. E.; Huang, C. C.; Jarvis, L. E.; Langridge, R. *J. Mol. Graphics* **1988**, 6, 13.
45. *CS Chemfinder Pro*, version 4.0; CambridgeSoft Corporation: 875 Massachusetts Avenue, Cambridge, MA 02139, USA, 1997.
46. Schapira, C. B.; Abasolo, M. I.; Perillo, I. A. *J. Heterocyclic Chem.* **1985**, 22, 577.
47. Case, D. A.; Pearlman, D. A.; Caldwell, J. W.; Cheatham, T. E. III; Ross, W. S.; Simmerling, C. L.; Darden, T. A.; Merz, K. M.; Stanton, R. V.; Cheng, A. L.; Vincent, J. J.; Crowley, M.; Ferguson, D. M.; Radmer, R. J.; Seibel, G. L.; Singh, U. C.; Weiner, P. K.; Kollman, P. A. *AMBER 5*; University of California: San Francisco, 1997.
48. Cornell, W. D.; Cieplak, P.; Bayly, C. I.; Gould, I. R.; Merz, K. M., Jr.; Ferguson, D. M.; Spellmeyer, D. C.; Fox, T.; Caldwell, J. W.; Kollman, P. A. *J. Am. Chem. Soc.* **1995**, 117, 5179.
49. Bayly, C. I.; Cieplak, P.; Cornell, W. D.; Kollman, P. A. *J. Phys. Chem.* **1993**, 97, 10269.
50. Cieplak, P.; Bayly, C. I.; Cornell, W. D.; Kollman, P. A. *J. Comput. Chem.* **1995**, 16, 1357.
51. Costantino, L.; Rastelli, G.; Vescovini, K.; Cignarella, G.; Vianello, P.; Del Corso, A.; Cappiello, M.; Mura, U.; Barlocco, D. *J. Med. Chem.* **1996**, 39, 4396.
52. Jorgensen, W. L.; Chandrasekhar, J.; Madura, J. P.; Impey, R. W.; Klein, M. L. *J. Chem. Phys.* **1983**, 79, 926.
53. Van Gunsteren, W. F.; Berendsen, H. J. C. *Mol. Phys.* **1977**, 34, 1311.
54. Beilstein, 6, III, 4450.
55. Beilstein, 6, IV, 5794.
56. Beilstein, 6, IV, 1746.
57. Beilstein, 6, IV, 1663.
58. Beilstein, 6, IV, 1694.
59. Sestany, K.; Bellini, F.; Fung, S.; Abraham, N.; Treasuryswala, A.; Humber, L.; Duquesne, N. S.; Dvornick, D. J. *Med. Chem.* **1984**, 27, 255.
60. Tallarida, R. J.; Murray, R. B. *Manual of Pharmacological Calculations with Computer Programs*, 2<sup>nd</sup> ed.; Springer: New York, 1987.